Sequential hole tunneling in n-type AlAs/GaAs resonant-tunneling structures from time-resolved photoluminescence

Chris Van Hoof

Interuniversity Microelectronics Center (IMEC), Kapeldreef 75, B-3001 Leuven, Belgium

Etienne Goovaerts

Physics Department, University of Antwerp (U.I.A.), Universiteitsplein 1, B-2610 Wilrijk-Antwerpen, Belgium

Gustaaf Borghs

Interuniversity Microelectronics Center (IMEC), Kapeldreef 75, B-3001 Leuven, Belgium

Time-resolved photoluminescence measurements on two n-type double-barrier AlAs/GaAs resonant tunneling structure devices under operation reveal that sequential tunneling of minority carriers governs the time dependence of the photoluminescence. Both the quantum well and the n^+-type GaAs emission reflect the hole transport from the accumulation layer into the quantum well and the escape through the second barrier, which is described in a three-level model. In the $L_B = 4$ nm barrier sample, transport rates are unchanged from $T = 80$ K to room temperature, which supports the tunneling character of the hole transport. Furthermore, the single barrier tunneling rate monotonously increases with applied electric field, and is much larger in a narrow-barrier device ($L_B = 3$ nm).

I. INTRODUCTION

Resonant tunneling has received special interest because of its importance both in fundamental physics and in practical high-speed device applications.[1] Since these devices are governed by majority-carrier electron transport, the determination of the electron charge build-up and the electron tunneling time is essential, and optical experiments have recently been applied to monitor these phenomena. Steady-state photoluminescence (PL) has been applied to determine the carrier accumulation near and inside the resonant tunneling structure (RTS).[2-7] Time-resolved PL experiments on unbiased RTS have revealed the electron and/or hole tunneling escape from the quantum well (QW) into the contact layers.[8-11] Few reports discuss the tunneling dynamics of photocreated minority-carrier holes in biased structures,[6,12] although the occurrence of non-negligible hole concentrations due to impact ionization has recently been established.[13] Furthermore, in heterojunction resonant tunneling light-emitting diodes, holes play an essential role.[14-16]

This paper therefore investigates the minority-carrier transport phenomena and their time scales in two n-type AlAs/GaAs RTS's with different barrier width.[17,18] It will be shown that the exciton time-resolved PL is governed by the simultaneous occurrence of a supply and an escape mechanism of holes in the QW, which is consistently described by rate equations in a three-level model. This model is further substantiated by the bias dependence of both the exciton and the n^+-type GaAs steady-state PL intensities. As a result, the rate for hole tunneling through a single barrier could be investigated as

a function of applied electric field, and for different temperatures and barrier widths.

II. EXPERIMENTAL PROCEDURES

The experiments reported here were performed on two RTS samples with a 6-nm GaAs well and AlAs barriers of thickness $L_B = 4$ and 3 nm for samples I and II, respectively. The samples were grown by molecular-beam epitaxy on a n^+-type silicon-doped GaAs substrate and consist of the following layers: 500-nm GaAs n^+-type (2×10^{18} cm^{-3}) buffer layer, 50-nm GaAs n-type (2×10^{16} cm^{-3}) spacer layer, an AlAs not-intentionally-doped (nid) barrier of thickness L_B, 6-nm GaAs nid well, an AlAs nid barrier of thickness L_B, 50-nm GaAs n-type (2×10^{16} cm^{-3}) spacer layer and 300-nm GaAs n^+-type (2×10^{18} cm^{-3}) contact layer. Standard lithography was used to define circular mesas that ranged in area between 400 and 2×10^4 μm^2. Fabrication involved hollow annular AuGe/Ni/Au Ohmic top contacts that allowed for optical probing under electric operation. The contact was connected to a bonding pad on top of a silicon nitride film that served for both isolation and passivation of the device mesas. The moderately small device area allows for the use of thinner barriers, leading to relatively high resonant current densities.

During low-temperature measurements the processed and packaged sample was mounted in a liquid-nitrogen-cooled Dewar and kept at a constant temperature of $T \approx 80$ K. Light from a synchronously pumped mode-locked dye laser (DCM, $\lambda = 680$ nm, pulse width < 5 ps)

was focused on the mesa. Neutral density filters reduced the average power density on the sample to levels at which no saturation effects could be observed, i.e., below $P_{exc} \approx 0.4$ W/cm^2. The luminescence was collected and dispersed in a 32-cm spectrometer, yielding 0.2-nm resolution, and detected with a cooled RCA31034 photomultiplier. Standard single-photon correlation techniques were employed to measure the PL decay. The 90% to 10% step of the falling tail of the instrumental function is smaller than 200 ps, which permits us to accurately resolve exponential decay times of down to ≈ 300 ps.

III. RESULTS

A. Spectral measurements

The current-voltage characteristics of both RTS, measured at 80 K are shown in Fig. 1(a). The PL spectra of the RTS under operation, which are shown in Fig. 2, resemble those of wider barrier samples in Refs. 2 and 7. Strictly speaking, the QW emission is not photoluminescence, but electro-photoluminescence,[6] since it originates from recombination of majority-carrier electrons and photocreated minority-carrier holes that are mainly created outside of the QW. The exciton PL intensity therefore contains both the variation in electron and hole accumulation inside the well.[19]
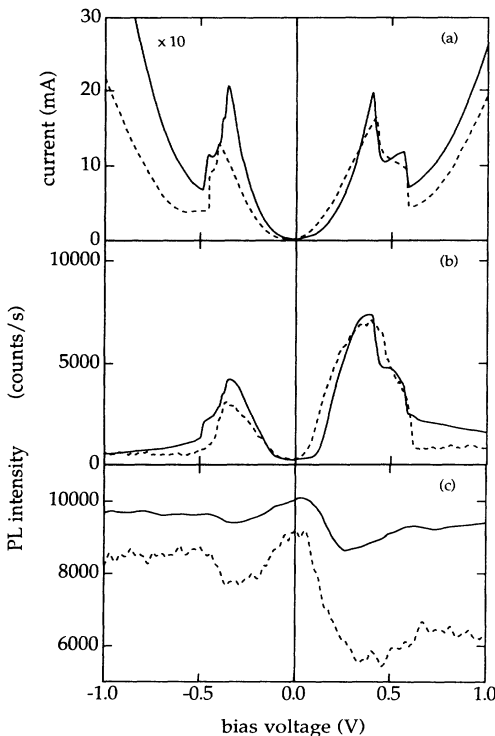
In our narrow-barrier samples and at sufficiently low

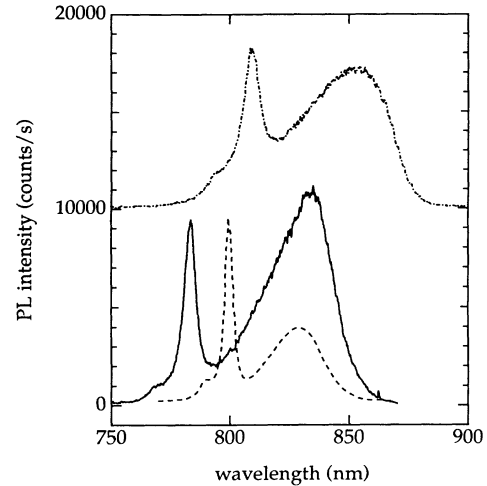FIG. 2. Photoemission spectrum measured at the electron tunneling resonance at $T = 80$ K for both samples (I in solid and II in dashed line), and at RT for sample I only (dotted line, shifted by 10^4 counts).

excitation power levels, the bias-dependent PL intensity of the QW exciton [Fig. 1(b)], mainly reflects the electron occupation, a similar correlation as previously reported.[2,3,5] In the region of the electron tunneling resonance an appreciable increase of the linewidth is observed,[17] which is more pronounced in sample II than in I. This results from electron accumulation in the QW, which is more important for the narrow- than for the wide-barrier sample. The bias dependence of the n^+-type GaAs PL intensity is shown in Fig. 1(c) and shows anticorrelation with the PL intensity of the confined exciton. While in sample I this represents only a small fraction, up to 40% of the n^+-type GaAs PL is lost at the peak voltage in sample II. This is discussed below in terms of hole trade-off between recombination in the n^+-type GaAs layers and in the QW.

Our PL spectra are strikingly dissimilar from previously reported measurements in the following aspects. A first qualitative difference is that, apart from the emission of the heavy-hole exciton, also that of the light-hole exciton can be resolved (Fig. 2). An important quantitative difference lies in the relative exciton PL intensity compared to that of the n^+-type GaAs PL: a relative peak value close to 1 in our samples, versus $\frac{1}{500}$ in structures with wider barriers.[19] This also allowed for the measurement of the confined-exciton PL at room temperature (RT), which to our knowledge has not been observed before. At the exciton transition the n^+-type GaAs contributes a background of about 20%. Due to the high relative intensity of exciton PL, we were able to observe the effect of hole tunneling through the RTS and recombination with electrons, both in the QW and in the n^+-type GaAs layer beyond it.

Several mechanisms can be responsible for the larger relative intensities of the exciton PL in our samples, resulting either from increase of the exciton PL intensity or from decrease of the n^+-type GaAs PL intensity. Different photoexcitation conditions are possibly involved,

FIG. 1. Bias dependence of (a) the current, and (b) and (c) the PL intensity from the confined exciton ($\lambda =783$ nm) and the n^+-type GaAs ($\lambda =820$ nm), respectively, measured at $T = 80$ K in samples I (solid line) and II (dashed line).

but this is not the most probable cause, since similar PL spectra have recently been observed for the pure electroluminescence of an identical RTS quenched in a p-n junction.[15,16] The two most probable causes are (1) the larger resonant tunneling current density—by a factor of 20 (200) in our RTS sample I (II) compared to Ref. 19—due to the narrower barriers, and (2) the more uniform electric field due to the smaller mesa dimensions.

B. Time-resolved experiments on sample I
(L_B=4 nm)

In Fig. 3 we present the time-dependent intensities of the confined exciton (solid lines) and the n^+-type GaAs (dashed line) PL, measured in sample I at 80 K. These curves are presented for three bias values: (a) below, (b) close to, and (c) well above the first electron tunneling resonance, which occurs at V_p=0.41 V.

The QW curves possess a measurable risetime of the order of 1 ns, much larger than expected from the instrumental response function (Fig. 3, dotted line). The low bias curves show a decay which is much slower than the single exponential decay of the n^+-type GaAs PL at zero bias, shown in Fig. 3(a) (thin solid line) for comparison. The slope of the long-time tail of the confined-exciton PL is clearly increasing with bias voltage (see also Sec. IV). At very low and very high bias, corresponding to relatively weak QW exciton emission, a sharply rising signal
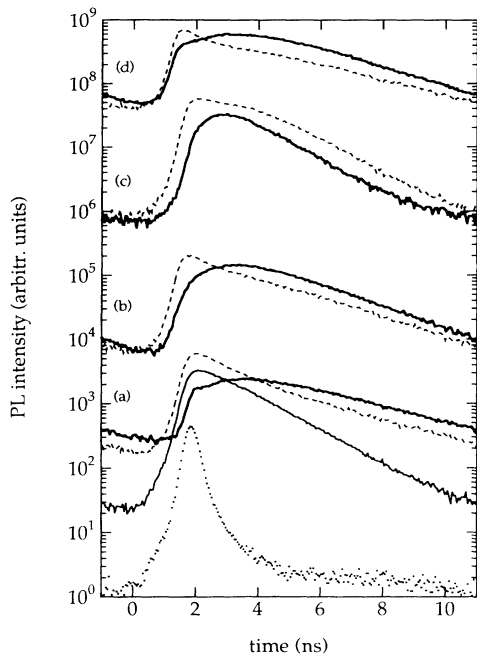

FIG. 3. Time-resolved PL measurements in sample I at T = 80 K and at different bias values, (a) V = 0.15 V, (b) V = 0.40 V, and (c) V = 0.90 V, which are below, at, and above the tunneling resonance, respectively. The rise and decay of the QW exciton (solid line) and n-type GaAs (dashed line) photoemission are clearly observed. Room-temperature results for sample I (V = 0.42 V) are shown in (d). The dotted line is the instrumental time response, and the thin solid line in (a) shows the zero bias, T = 80 K decay curve of the n-type GaAs PL.

is superimposed on this curve. A close inspection of the spectral and time-resolved measurements shows that it is originating from the tail intensity of the broad n^+-type GaAs emission at the energy of the confined-exciton transition.

The spectral measurements have demonstrated the competition between recombination of holes inside and outside of the well. More information is gained from time-resolved measurements in the n^+-type GaAs emission band. The zero bias measurement [Fig. 3(a), thin solid line] shows a single exponential decay [$\tau_g(0)$=1.53 ns at 80 K] and a risetime corresponding to the instrumental response. At increasing bias voltage a new component adds to this signal [see Figs. 3(a)–3(c), dashed lines], which is very similar to the time-dependent confined-exciton signal. In particular, the same slope is observed for the long-time tail and it possesses a similar risetime. At high bias voltage this component even becomes larger in integrated intensity than the fast-rising component. Reabsorption of confined-exciton PL in the n^+-type GaAs layers should be discarded as an explanation for the delayed PL component: The bias dependence of the time-integrated intensity of this component is not correlated to the intensity of the confined-exciton PL. It is continuously increasing with bias, and becomes more important than the direct contribution beyond the valley voltage, $V > V_v$ = 0.60 V.

In addition to the low-temperature measurements discussed until now, it was possible in this sample to perform experiments at RT. The same qualitative features are observed, as is shown in Fig. 3(d). Despite the much higher n^+-type GaAs background, the rise and decay of the exciton PL is still clearly observed. Also in the decay curves, the contribution of holes tunneling through the whole RTS structures is still obvious and it can easily be distinguished from the direct contribution [$\tau_g(0)$ = 1.34 ns at RT]. The RT measurements turn out to be crucial in the identification of the hole transport as a tunneling process (see Sec. V).

C. Time-resolved experiments on sample II
(L_B=3 nm)

The time dependence of the confined exciton and n^+-type GaAs PL in sample II at V_p= 0.40 V is shown in Fig. 4. The decay of the n^+-type GaAs emission is very fast [$\tau_g(0)$ = 0.46 ns at V= 0 and T = 80 K] due to the higher Si doping level. At all bias values up to the valley V_v, the response of the confined-exciton PL is distinctly slower than that of the n-type GaAs emission. Nevertheless, the confined exciton is decaying much faster than in sample I, which is consistent with a faster tunneling of the holes through the narrower barriers.

In this sample, the shape of the n^+-type GaAs decay curve is not changing with increasing bias, and no indication is found for a PL contribution from holes that would have tunneled through the whole RTS before recombining in the contact layers (see also Sec. IV B). This qualitative difference compared to sample I results from the smaller barrier width and from the shorter recombination time τ_g.
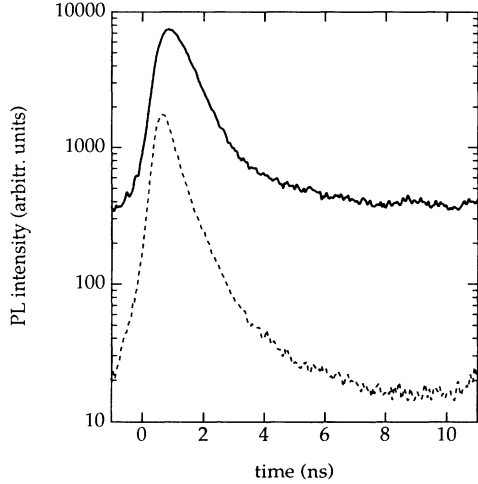
FIG. 4. Time-resolved PL measurements in sample II at $T = 80$ K at the electron tunneling resonance, $V = 0.41$ V, showing the signals from the QW (solid line) and from the n^+-type GaAs layers (dashed line).
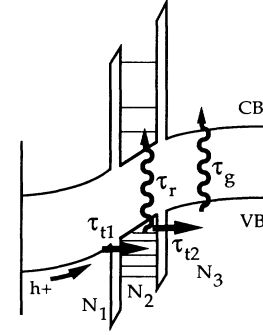

FIG. 5. Schematic band diagram of the RTS devices indicating the transition rates and the hole populations involved in the three-level model.

First, the narrower barriers of the RTS ($L_B = 3$ nm) lead to a tenfold increase of the electron current density compared to sample I [see Fig. 1(a)] and to a higher electron accumulation inside the well. This leads to a higher probability for recombination in the well, which is witnessed [Fig. 1(c)] by the higher loss of n^+-type GaAs PL intensity in this sample. In the most effective case, i.e., holes moving from the surface to the substrate, this loss reaches 40% compared to about 10% in sample I. The loss in PL is even more dramatic since the holes created below the RTS (i.e., $\frac{1}{3}$ of the total amount of holes) do not participate in the tunneling processes.

Second, the very fast electron-hole recombination in the contact layers competes with the accumulation of holes against the first barrier of the RTS, and only a reduced amount of holes reaches the hole accumulation layer. In conclusion we can estimate that a fraction appreciably smaller than 30% of the total hole production can contribute to n^+-type GaAs emission after tunneling through the whole RTS.

IV. MODEL AND ANALYSIS OF THE DATA

A. Three-level model and rate equations

The time behavior of both the QW and n^+-type GaAs emission can be explained in a natural and consistent way by the following model, in which hole tunneling plays an essential role. Since electrophotoluminescence of the RTS is measured, and the contribution of the photocreated electrons to the total current is negligible, the time evolution of the PL must completely follow from the dynamics of the hole population in the different layers of the device (see Fig. 5). Immediately after photoexcitation an appreciable part of the holes created in the n- and n^+-type GaAs layers will accumulate against the AlAs barrier—upper or lower barrier depending on the polar-

ity of the electric field—as a result of diffusive motion, which is too fast to be observed in our experiments. From the diffusion constant and the minority-carrier mobility[20] at $T = 80$ K, the accumulation time is estimated to be less than 0.4 ns, comparable to our time resolution. This may affect the measurements on sample II, for which fast response times have been observed (Sec. III C). From the accumulation layer, holes can tunnel through the first barrier into the QW at a rate τ_{t1}^{-1}, where they can either recombine inside the QW as a confined exciton with a probability τ_r^{-1} per time unit, or escape through the second barrier at a rate τ_{t2}^{-1} in the electron-emitting n-type GaAs layer. In this layer electron-hole recombination occurs after a time τ_g. In such a model the following rate equations describe the time evolution of the hole populations:

$$\frac{dN_1}{dt} = -\frac{N_1}{\tau_{t1}} \quad ,$$

$$\frac{dN_2}{dt} = \frac{N_1}{\tau_{t1}} - \left(\frac{1}{\tau_r} + \frac{1}{\tau_{t2}}\right) N_2 \quad , \tag{1}$$

$$\frac{dN_3}{dt} = \frac{N_2}{\tau_{t2}} - \frac{N_3}{\tau_g},$$

in which N_1 and N_2 represent the population of holes in the accumulation layer and in the QW, respectively, while N_3 is the number of holes which have reached the n-type GaAs layer after tunneling through the RTS. Creation of holes directly inside the QW yields a very small contribution to the exciton PL, which we neglect, and therefore $N_2(t = 0) = N_3(t = 0) = 0$. Although this set of linear differential equations can be readily solved, the analytical form of the solutions depends on the values of the time constants.

After Laplace transformation a set of algebraic equations has to be solved, using the appropriate initial conditions $N_1(s = 0) = N_{10}$ and $N_2(s = 0) = N_3(s = 0) = 0$, where N_{10} is the number of initially accumulated holes. This yields the solutions:

$$N_1(s) = \frac{N_{10}}{s + \dfrac{1}{\tau_{t1}}},$$

$$N_2(s) = \frac{N_{10}}{\tau_{t1}\left(s + \dfrac{1}{\tau_{t1}}\right)\left(s + \dfrac{1}{\tau_r} + \dfrac{1}{\tau_{t2}}\right)},$$

$$N_3(s) = \frac{N_{10}}{\tau_{t1}\tau_{t2}\left(s + \dfrac{1}{\tau_{t1}}\right)\left(s + \dfrac{1}{\tau_r} + \dfrac{1}{\tau_{t2}}\right)\left(s + \dfrac{1}{\tau_g}\right)},$$

in which the distinction between the cases becomes more obvious. If the real poles of the functions N_i are all different from each other, the solutions are linear combinations of single exponentials with the corresponding decay rates,

$$N_1(t) = N_{10}e^{-t/\tau_{t1}}, \tag{2}$$

$$N_2(t) = \frac{N_{10}}{\tau_{t1}\left(\dfrac{1}{\tau_r} + \dfrac{1}{\tau_{t2}} - \dfrac{1}{\tau_{t1}}\right)}(e^{-t/\tau_{t1}} - e^{-(1/\tau_r + 1/\tau_{t2})t}), \tag{3}$$

$$N_3(t) = N\left[\left(\frac{1}{\tau_r} + \frac{1}{\tau_{t2}} - \frac{1}{\tau_g}\right)e^{-t/\tau_{t1}} \right.$$
$$+ \left(\frac{1}{\tau_g} - \frac{1}{\tau_{t1}}\right)e^{-(1/\tau_r + 1/\tau_{t2})t}$$
$$\left. - \left(\frac{1}{\tau_r} + \frac{1}{\tau_{t2}} - \frac{1}{\tau_{t1}}\right)e^{-t/\tau_g} \right], \tag{4}$$

where

$$N = N_{10}\frac{1}{\tau_{t1}\tau_{t2}\left(\dfrac{1}{\tau_r} + \dfrac{1}{\tau_{t2}} - \dfrac{1}{\tau_g}\right)\left(\dfrac{1}{\tau_g} - \dfrac{1}{\tau_{t1}}\right)\left(\dfrac{1}{\tau_r} + \dfrac{1}{\tau_{t2}} - \dfrac{1}{\tau_{t1}}\right)}.$$

Let us consider the limiting case

$$\frac{1}{\tau_t} = \frac{1}{\tau_{t1}} = \frac{1}{\tau_{t2}} \approx \frac{1}{\tau_r} + \frac{1}{\tau_{t2}}, \tag{5}$$

which will in the analysis turn out to be appropriate for the case of sample I. It results from the assumptions of equal tunneling times through the first and second barrier, and of negligible recombination rate. In this case Eqs. (3) and (4) reduce to

$$N_2(t) = \frac{N_{10}}{\tau_t}te^{-t/\tau_t}, \tag{6}$$

$$N_3(t) = \frac{N_{10}}{\tau_t^2\left(\dfrac{1}{\tau_t} - \dfrac{1}{\tau_g}\right)^2}\left[e^{-t/\tau_g} - \left(\frac{1}{\tau_t} - \frac{1}{\tau_g}\right)te^{-t/\tau_t} \right.$$
$$\left. - e^{-t/\tau_t} \right], \tag{7}$$

The solution (3) for $N_2(t)$ is shown in Fig. 6 for two sets of time constants. A clear risetime is observed for N_2, being the shorter of τ_{t1} and $(\tau_r^{-1} + \tau_{t2}^{-1})^{-1}$, followed by a decay which only for large times turns into an exponential form, with a decay time that is the larger of these two time constants. From the shape of this curve it is clear that substantial errors can be made if the tail is approximated by a single exponential function. Not shown is $N_3(t)$ which also shows a risetime, reaches a maximum at later times than N_2, and then slowly evolves into a near-to-exponential decay.

In all cases the risetime (decay) is the shortest (longest) of the time constants involved, and as a consequence it is not necessarily connected to the supply (escape) mech-

anism. This is clarified by the examples in this figure: $N_2(t)$ is given for $\tau_{t1} = 2.5$ ns and $(\tau_r^{-1} + \tau_{t2}^{-1})^{-1} = 1.5$ ns (solid line), and the same result, apart from a scaling factor, is obtained for the switched values $\tau_{t1} = 1.5$ ns and $(\tau_r^{-1} + \tau_{t2}^{-1})^{-1} = 2.5$ ns (dashed line). Apart from a scaling factor, both functions are identical. The case of equal source and drain time constants, $\tau_{t1} = (\tau_r^{-1} + \tau_{t2}^{-1})^{-1} =$
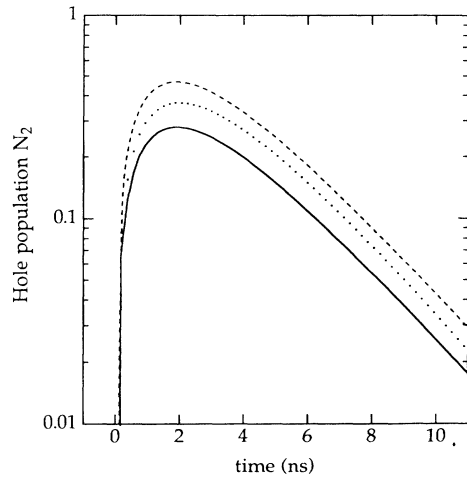
FIG. 6. Solutions of the rate equations (1) for N_2, the hole population in the QW, are shown for several sets of time constants: The solid line results for $\tau_{t1} = 2.5$ ns and $(\tau_r^{-1} + \tau_{t2}^{-1})^{-1} = 1.5$ ns. The same solution, except for a constant factor, is obtained for $N_2(t)$ after exchanging the rates, $\tau_{t1} = 1.5$ ns and $(\tau_r^{-1} + \tau_{t2}^{-1})^{-1} = 2.5$ ns (dashed line). The case of equal rates for the source and drain term of holes in the well is illustrated by the dotted curve, for $\tau_{t1} = (\tau_r^{-1} + \tau_{t2}^{-1})^{-1} = 2$ ns.

2 ns, follows from Eq. (6) and leads to a very similar time dependence (dotted line in Fig. 6) of the hole population in the well.

B. Analysis of the time-dependent PL signals

The time-resolved PL measurements have been analyzed using the above rate equations, taking into account the following additional effects.

(1) The signal of the confined-exciton PL contains a tail contribution from the n^+-type GaAs PL. The latter is small ($< 5\%$) at the peak bias voltage V_p but becomes relatively more important at very low and at high applied voltages [see Fig. 1(b)]. It was possible to estimate the ratio of both contributions from the spectral measurements.

(2) Besides the contribution described by (4) or (7) from holes which have tunneled through the whole structure, the n^+-type GaAs PL also consists of a direct part, with a single exponential decay with radiative lifetime τ_g. This yields an additional fitting parameter α, which represents the relative importance of the former contribution.

(3) Because of the short period between exciting pulses ($\Delta \approx 12.2$ ns) and the relatively slow decay of the PL, the accumulation of signal originating from preceding pulses is substantial. Fortunately, the summation over preceding periods of the functions appearing in (2)–(7) can be treated analytically.

(4) In order to obtain a detailed comparison of experimental and calculated curves, it is imperative to make the convolution of the latter with the instrumental resolution function.

Fitting the resulting curves to the experimental data was performed by χ^2 minimalization, taking $\sigma = \sqrt{N}$ as the variance on the accumulated counts N.

For sample I it was possible to first analyze the QW emission separately at bias values around V_p, because of the very small n^+-type GaAs background. Initially, different risetimes and decay times were employed [Eqs. (3) and (4)], but this leads in many cases to nearly equal values for the time constants. Also, equally good results were obtained when equal time constants were *a priori* assumed [Eqs. (6) and (7)]. Therefore we concluded that for sample I the conditions (5) are closely valid (see Sec. V), and the data have been further analyzed on this basis.

In Fig. 7 we compare the experimental results with the calculated PL curves, obtained from a simultaneous fitting of the confined-exciton and n^+-type GaAs PL. For each of the signals, the weighed residuals between experimental and calculated curves are shown. Such an analysis was systematically performed for the wide-barrier sample I at $T = 80$ K and at RT. The resulting time constant τ_t for single-barrier tunneling is shown in Fig. 8(a) as a function of bias voltage. The fraction of holes α contributing to the n^+-type GaAs PL after tunneling through the RTS, is given as a function of bias in Fig. 8(b). At low bias voltage, α is small, because in the relatively small electric field only part of the holes created above the RTS are accumulating against the first
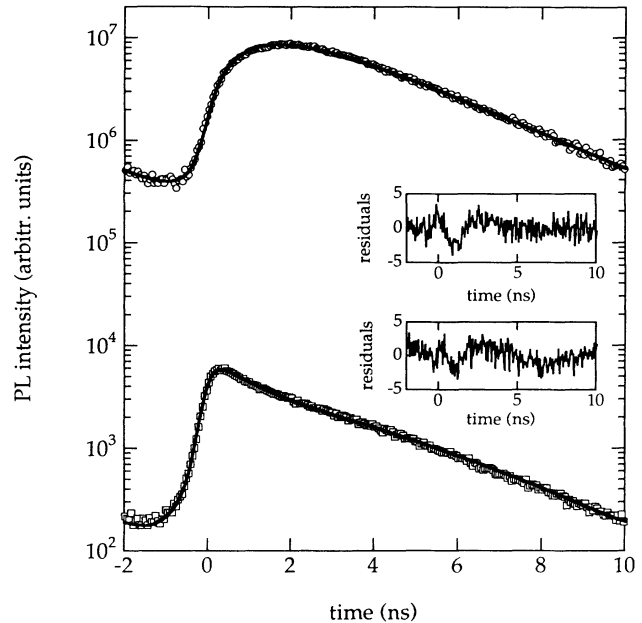

FIG. 7. Illustration of the fitting procedure for sample I at $T = 80$ K and $V = 0.40$ V. The parameter values were obtained from the fitting procedure described in Sec. IV B, which yields the constants $\tau_t = (1.61 \pm 0.01)$ ns and $\tau_g = (1.15 \pm 0.07)$ ns, and the tunneling contribution to the n-type GaAs PL $\alpha = (0.40 \pm 0.02)$. The experimental time-dependent signals of the confined-exciton (o) and the n-type GaAs ($\square$) PL, are compared with the calculated curves (solid lines), and the weighed residuals are shown in the insets.

barrier. At V_v, one approaches $\alpha = \frac{2}{3}$, which is expected for efficient accumulation and tunneling of the holes. A monotonous increase of α would be expected between these two regions, but the actual curve [Fig. 8(b)] is depressed in the region of resonant tunneling by an amount roughly proportional to the confined-exciton PL [Fig. 1(b)]. This loss results from radiative recombination of holes in the quantum well, which will be further discussed in Sec. V. In the fitting procedure, it was necessary to treat the n^+-type GaAs lifetime τ_g as a variable parameter, and the substantial decrease of τ_g for increasing bias is also shown in Fig. 8(c). The most probable cause for this effect is faster e-h recombination in the n-type GaAs layer beyond the RTS, which is also the electron accumulation layer in which the electron density increases with electric field. Because of the fast diffusive motion, the holes in the second n^+-type GaAs layer all spend part of their time in this electron accumulation region, which leads to an overall decrease of the recombination time τ_g. The downward jump of τ_g in the region of negative differential resistivity is compatible with the expected increase of electron accumulation in the electron emitting contact layer.

The short time constants involved in the time-resolved PL spectra of sample II ($L_B = 3$ nm) are close to the experimental resolution, but compatibility with the proposed model can be investigated. Taking into account
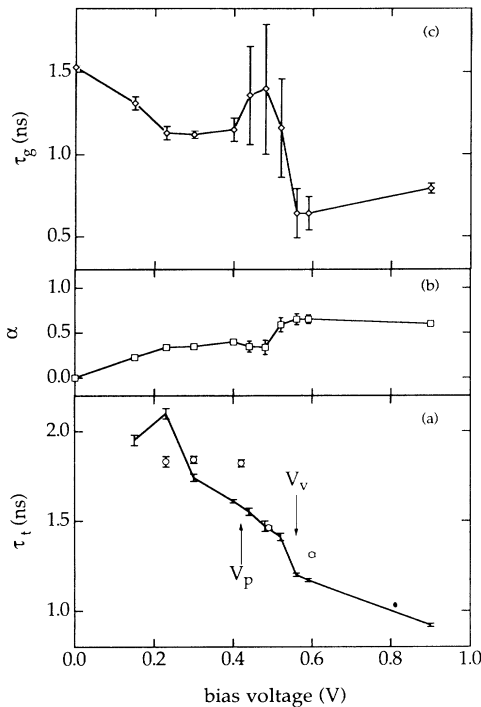
FIG. 8. (a) Tunneling time τ_t derived from the three-level model analysis (Sec. IV) for the 4-nm barrier sample I at $T = 80$ K (connected by a solid line) and at room temperature (o). The $T = 80$ K values of the peak (V_p) and valley (V_v) voltage are indicated. (b) Relative contribution of tunneling holes to the n-type GaAs PL intensity α, and (c) n-type GaAs recombination lifetime τ_g.

the effects of strong electron accumulation discussed in Sec. III C, the recombination rate in the QW is not negligible and therefore the condition (5) is not valid in this case. If the recombination rate is appreciably larger than the tunneling rate, this will lead to a fast rise of the QW emission, and a slower decay determined by the exponentially decreasing supply from the accumulation layer. Acceptable fits of the confined-exciton PL curves are obtained using (3) for a range of values of the rise-time $0.2 < \tau_{\mathrm{rise}} < 0.5$ ns, taking equal tunneling times $\tau_t = \tau_{t1} = \tau_{t2}$ and $\tau_{\mathrm{rise}} = (\frac{1}{\tau_r} + \frac{1}{\tau_t})^{-1}$. This always results in tunneling times shorter than 1 ns. Accurate fits at all bias values were obtained for $\tau_{\mathrm{rise}} = 0.30$ ns, which yield a tunneling time decreasing from $\tau_t = 0.80$ ns to 0.52 ns when the bias increases from 0.15 to 0.60 V, respectively. It is not excluded that the risetime is partly resulting from the finite time needed for accumulation of the holes outside the first barrier. The decay of the n^+-type GaAs emission is hardly affected by the bias voltage, and a single exponential analysis yields a decay time close to the already small zero bias value of $\tau_g(0) = 0.46$ ns. A combined analysis of QW and n^+-type GaAs signals was performed using Eqs. (3) and (4) in order to obtain an upper limit for the indirect contribution by holes that have first traveled through the whole RTS. While a small indirect contribution of about 10% slightly improves the quality of the fit, a value over 20% leads to unrealistic

deviations between experimental and calculated curves. This low fraction of holes tunneling through the whole RTS is acceptable only if indeed the recombination rate inside the QW is appreciably larger than the tunneling escape rate.

V. DISCUSSION

The model and rate equations presented in Sec. IV A give a satisfactory description of the time-dependent PL measurements in our two samples with different barrier thickness, and for different conditions of bias voltage and temperature. The resulting rate for crossing of the AlAs barrier is unchanged between $T = 80$ K and room temperature and this strongly supports that this is a tunneling process, and not a thermally activated one. Tunneling of a single barrier by a particle under an applied electric field[21] is also compatible with the monotonous increase of the tunneling rate observed with increasing bias voltage, and its drastic enhancement from a 4-nm to a 3-nm barrier width. Analogous results were found for electron escape from a QW in an applied electric field[22] for different barrier widths.

One more aspect can be quantitatively considered in relation with the proposed model, i.e., the changes in n^+-type GaAs PL intensity as a function of bias voltage, shown in Fig. 1(c). The ratio of holes created above and below the RTS can be estimated from the relative amount of confined-exciton PL for positive over negative bias [see Fig. 1(b)], which is around 2:1 for both samples at $T = 80$ K. Approximately the same ratio is observed between opposite bias polarities for the loss of n^+-type GaAs PL around V_p [Fig. 1(c)]. Consider the positive bias case, when holes from the surface contact layer ($\frac{2}{3}$ of the total amount) accumulate against the RTS. One can estimate the radiative decay rate in the QW from the relative decrease of the n^+-type GaAs PL at the resonance, in the assumption that the latter results solely from tradeoff with recombination in the QW, and neglecting nonradiative decay and other alternative mechanisms of e-h recombination. The maximum 10% decrease of n^+-type GaAs PL in sample I then means that about $\frac{1}{7}$ of the holes tunneling through the first barrier are disappearing in the well by radiative exciton decay. This leads to an estimate of $\tau_t^{-1} \approx 6 \times \tau_r^{-1}$ at the maximum of the electron tunneling current and accumulation in the well. This independent observation confirms that the rate of radiative recombination in the QW is small compared to that of tunneling escape, and that the conditions (5) hold in reasonable approximation. The same estimation for sample II $(L_B = 3$ nm) yields a different result: A decrease of up to 40% of n^+-type GaAs PL means that nearly $\frac{2}{3}$ of the tunneling holes disappear radiatively in the QW, and $\tau_t^{-1} \approx \frac{1}{2} \times \tau_r^{-1}$. In agreement with the analysis performed for the time-resolved measurements of sample II, the radiative recombination rate is more important than the tunneling rate. In this case, we probably are overestimating the fraction of holes accumulating against the first barrier, since the competing process of fast radiative recombination (Secs. III C and IV B) in the highly doped contact layer was not accounted for.

VI. SUMMARY AND CONCLUSION

In this work, spectral and time-resolved PL measurements have been combined to obtain a detailed picture of the transport of minority holes in *n*-type resonant tunneling devices under operation.

The PL intensity of the QW exciton was shown to be directly correlated to the electron tunneling current [Figs. 1(a) and 1(b)], more specifically, the resonant part of this current. The asymmetry in the PL intensity curve for positive versus negative bias follows trivially from the finite penetration depth of the exciting light. However, the anticorrelation between the *n*-type GaAs and the QW emission intensities is a clear indication for the existence of a tradeoff mechanism between the electron-hole recombination inside and outside the well. Finally, the spectral measurements give a measure of the amount of electron accumulation in the QW, through the sizable line broadening of the exciton transition in the first resonance region.

The time-resolved PL measurements have provided more direct information about the hole motion after photocreation. The nanosecond rise and decay of the QW emission, and the additional contribution developing with increasing bias on top of the exponential *n*-type GaAs PL decay, have been analyzed using the rate equations in a simple three-level model. For both samples, the relative importance was estimated of radiative decay in the QW and recombination in the *n*-type GaAs layers after passing through the whole RTS. Mutually consistent conclusions concerning this point were independently drawn from either the time-averaged intensity measurements or the analysis of the time-resolved experiments.

Measurements at $T = 80$ K and at RT in two RTS samples with different barrier widths (L_B=4 and 3 nm), under applied bias, led us to the following conclusions. After very fast diffusive motion and trapping at the AlAs barrier, the holes sequentially tunnel through the two barriers of the RTS. Passing through the QW, part of the holes form confined excitons which decay radiatively, and the remaining holes recombine in the accumulation layer of the electron-emitting contact layer. The tunneling nature of the barrier crossing was demonstrated by comparison of $T = 80$ K and RT experiments in sample I, yielding nearly equal time constants at all bias values. In this way, we were able to directly determine the hole tunneling rate as a function of applied bias. A monotonous increase of the tunneling rate with increasing bias voltage is observed, as expected for a charged particle tunneling through a barrier in an increasing electrical field. Consistently, much larger tunneling rates are observed in the narrow-barrier (II) than in the wide-barrier (I) sample.

ACKNOWLEDGMENTS

[1]*Physics of Quantum Electron Devices*, edited by Federico Capasso, Springer Series in Electronics and Photonics Vol. 28 (Springer-Verlag, Berlin, 1990).

[2]J.F. Yung, B.M. Wood, G.C. Aers, R.L.S. Devine, H.C. Liu, D. Landheer, M. Buchanan, A.J. SpringThorpe, and P. Mandeville, Phys. Rev. Lett. **60**, 2085 (1988).

[3]J.F. Young, B.M. Wood, G.C. Aers, R.L.S. Devine, H.C. Liu, M. Buchanan, A.J. SpringThorpe, and P. Mandeville, Superlatt. Microstruct. **5**, 411 (1989).

[4]L. Eaves, M.L. Leadbeater, D.G. Hayes, E.S. Alves, F.W. Sheard, G.A. Toombs, P.E. Simmonds, M.S. Skolnick, M. Henini, and O.H. Hughes, Solid-State Electron. **32**, 1101 (1989).

[5]N. Vodjdani, F. Chevoir, D. Thomas, D. Cote, P. Bois, E. Costard, and S. Delaitre, Appl. Phys. Lett. **55**, 1528 (1989).

[6]N. Vodjdani, D. Cote, D. Thomas, B. Sermage, P. Bois, E. Costard, and J. Nagle, Appl. Phys. Lett. **56**, 33 (1990).

[7]H. Yoshimura, J.L. Schulman, and H. Sakaki, Phys. Rev. Lett. **64**, 2422 (1990).

[8]M. Tsuchiya, T. Matsusue, and H. Sakaki, Phys. Rev. Lett. **59**, 2356 (1987).

[9]M. Tsuchiya, T. Matsusue, and H. Sakaki, in *Ultrafast Phenomena VI*, edited by T. Yajima, K. Yoshihara, C.B. Harris, and S. Shionoya, Springer Series in Chemical Physics Vol. 48 (Springer-Verlag, Berlin, 1988), p. 304.

[10]M.K. Jackson, M.B. Johnson, D.H. Chow, and T.C. McGill, Appl. Phys. Lett. **54**, 552 (1989).

[11]E.T. Yu, M.K. Jackson, and T.C. McGill, Appl. Phys. Lett. **55**, 744 (1989).

[12]S. Charbonneau, J.F. Young, and A.J. SpringThorpe, Appl. Phys. Lett. **57**, 264 (1990).

[13]C.R.H. White, M.S. Skolnick, L. Eaves, M.L. Leadbeater, M. Henini, G. Hill, O.H. Hughes, and M.A. Pate, Superlatt. Microstruct. **8**, 391 (1990).

[14]L. Eaves, in *Proceedings of ESSDERC91* [Microelectron. Eng. **15**, 661 (1991)].

[15]C. Van Hoof, J. Genoe, E. Goovaerts, R. Mertens, and G. Borghs, Electron. Lett. **28**, 123 (1992).

[16]C. Van Hoof, J. Genoe, R. Mertens, G. Borghs, and E. Goovaerts, Appl. Phys. Lett. **60**, 77 (1992).

[17]C. Van Hoof, E. Goovaerts, and G. Borghs, Proc. SPIE **1362**, 291 (1990).

[18]E. Goovaerts, C. Van Hoof, and G. Borghs, Physica B **175**, 307 (1991).

[19]M.S. Skolnick, P.E. Simmonds, D.G. Hayes, G.W. Smith, A.D. Pitt, C.R. Whitehouse, H.J. Hutchinson, C.R.H. White, L. Eaves, M. Henini, and O.H. Hughes, Phys. Rev. B **42**, 3069 (1990).

[20]C. Goradia, M. Ghalla-Goradia, and H. Curtis, in *Proceedings of the 17th IEEE Photovoltaic Specialists Conference* (Kissimmee, FL, 1984), edited by L. Ralph (IEEE, 1984), p. 56.

[21]L.D. Landau and E.M. Lifshitz, *Quantum Mechanics, Non-Relativistic Theory*, 3rd ed. (Pergamon, New York, 1977), pp. 178–181.

[22]T.B. Norris, X.J. Song, W.J. Schaff, L.F. Eastman, G. Wicks, and G.A. Mourou, Appl. Phys. Lett. **54**, 60 (1989).